Article

Vertical full-colour micro-LEDs via 2D materials-based layer transfer

https://doi.org/10.1038/s41586-022-05612-1

Received: 16 January 2022

Accepted: 30 November 2022

Published online: 1 February 2023

Check for updates

Jiho Shin[1,2,3,16], Hyunseok Kim[1,2,16], Suresh Sundaram[4,16], Junseok Jeong[1,2,5,16], Bo-In Park[1,2], Celesta S. Chang[1,2], Joonghoon Choi[5], Taemin Kim[6], Mayuran Saravanapavanantham[2,7], Kuangye Lu[1,2], Sungkyu Kim[1,2,5], Jun Min Suh[1,2], Ki Seok Kim[1,2], Min-Kyu Song[1,2], Yunpeng Liu[1,2], Kuan Qiao[1,2], Jae Hwan Kim[1,2], Yeongin Kim[1,2,8], Ji-Hoon Kang[1,2], Jekyung Kim[1,2], Doeon Lee[9], Jaeyong Lee[1,2], Justin S. Kim[10], Han Eol Lee[1,2,11], Hanwool Yeon[1,2,12], Hyun S. Kum[1,2,6], Sang-Hoon Bae[1,2,10], Vladimir Bulovic[2,7], Ki Jun Yu[6], Kyusang Lee[9] ✉, Kwanghun Chung[3,13] ✉, Young Joon Hong[5] ✉, Abdallah Ougazzaden[4,14] ✉ & Jeehwan Kim[1,2,15] ✉

Micro-LEDs (μLEDs) have been explored for augmented and virtual reality display applications that require extremely high pixels per inch and luminance[1,2]. However, conventional manufacturing processes based on the lateral assembly of red, green and blue (RGB) μLEDs have limitations in enhancing pixel density[3–6]. Recent demonstrations of vertical μLED displays have attempted to address this issue by stacking freestanding RGB LED membranes and fabricating top-down[7–14], but minimization of the lateral dimensions of stacked μLEDs has been difficult. Here we report full-colour, vertically stacked μLEDs that achieve, to our knowledge, the highest array density (5,100 pixels per inch) and the smallest size (4 μm) reported to date. This is enabled by a two-dimensional materials-based layer transfer technique[15–18] that allows the growth of RGB LEDs of near-submicron thickness on two-dimensional material-coated substrates via remote or van der Waals epitaxy, mechanical release and stacking of LEDs, followed by top-down fabrication. The smallest-ever stack height of around 9 μm is the key enabler for record high μLED array density. We also demonstrate vertical integration of blue μLEDs with silicon membrane transistors for active matrix operation. These results establish routes to creating full-colour μLED displays for augmented and virtual reality, while also offering a generalizable platform for broader classes of three-dimensional integrated devices.

Micro-light-emitting diodes (μLEDs) are considered ideal building blocks for augmented and virtual reality (AR/VR) displays owing to their small size and high level of brightness, which are crucial for near-eye and/or outdoor applications[1,2]. However, the realization of full-colour μLED displays via conventional mass transfer processes has been challenging. These processes require the extraction of red, green and blue (RGB) μLED chips from their respective epitaxial wafers—GaAs for red, and sapphire for green and blue LEDs, for example—followed by consecutive precision transfers of R-, G- and B-LED chips for lateral assembly of RGB pixels[19,20]. Despite enormous improvement in resolution, yield and throughput, these approaches have yet to yield μLED displays of sufficiently high pixel density.

To address these issues, many researchers have developed μLED displays with vertically aligned RGB subpixels through monolithic integration of freestanding RGB LED membranes followed by top-down fabrication[7–14]. However, conventional epitaxial lift-off techniques for the production of freestanding LEDs can be inadequate for construction of the sub-10 μm pixels required for AR/VR displays[21]. Specifically, conventional heteroepitaxy and laser lift-off processes for indium gallium nitride (InGaN)-based LEDs require a thick buffer under the active layers to minimize lattice mismatch-induced dislocations[22] and prevent laser-induced damage[23], respectively. As a result, these LED films are 5–10 μm in thickness, which makes the fabrication of sub-10 μm vertical μLEDs impractical because the high aspect ratio impedes high-resolution lithography. Slow rates of release processes and limited reuse of costly wafers present additional concerns for manufacturers. Consequently, there is a critical need for a lift-off technique that can yield freestanding LED membranes that are ultrathin, readily

[1]Department of Mechanical Engineering, Massachusetts Institute of Technology, Cambridge, MA, USA. [2]Research Laboratory of Electronics, Massachusetts Institute of Technology, Cambridge, MA, USA. [3]Department of Chemical Engineering, Massachusetts Institute of Technology, Cambridge, MA, USA. [4]CNRS, IRL 2958, GT–CNRS, Georgia Tech-Lorraine, Metz, France. [5]Department of Nanotechnology and Advanced Materials Engineering, Sejong University, Seoul, Republic of Korea. [6]Department of Electrical and Electronic Engineering, Yonsei University, Seoul, Republic of Korea. [7]Department of Electrical Engineering and Computer Science, Massachusetts Institute of Technology, Cambridge, MA, USA. [8]Department of Electrical Engineering and Computer Science, University of Cincinnati, Cincinnati, OH, USA. [9]Department of Electrical and Computer Engineering, University of Virginia, Charlottesville, VA, USA. [10]Department of Mechanical Engineering and Materials Science, Washington University in Saint Louis, St. Louis, MO, USA. [11]Division of Advanced Materials Engineering, Jeonbuk National University, Jeonju, Republic of Korea. [12]School of Materials Science and Engineering, Gwangju Institute of Science and Technology, Gwangju, Republic of Korea. [13]Institute for Medical Engineering and Science, Massachusetts Institute of Technology, Cambridge, MA, USA. [14]School of Electrical and Computer Engineering, Georgia Institute of Technology, Atlanta, GA, USA. [15]Department of Materials Science and Engineering, Massachusetts Institute of Technology, Cambridge, MA, USA. [16]These authors contributed equally: Jiho Shin, Hyunseok Kim, Suresh Sundaram, Junseok Jeong. ✉e-mail: kyusang@virginia.edu; khchung@mit.edu; yjhong@sejong.ac.kr; abdallah.ougazzaden@georgiatech-metz.fr; jeehwan@mit.edu

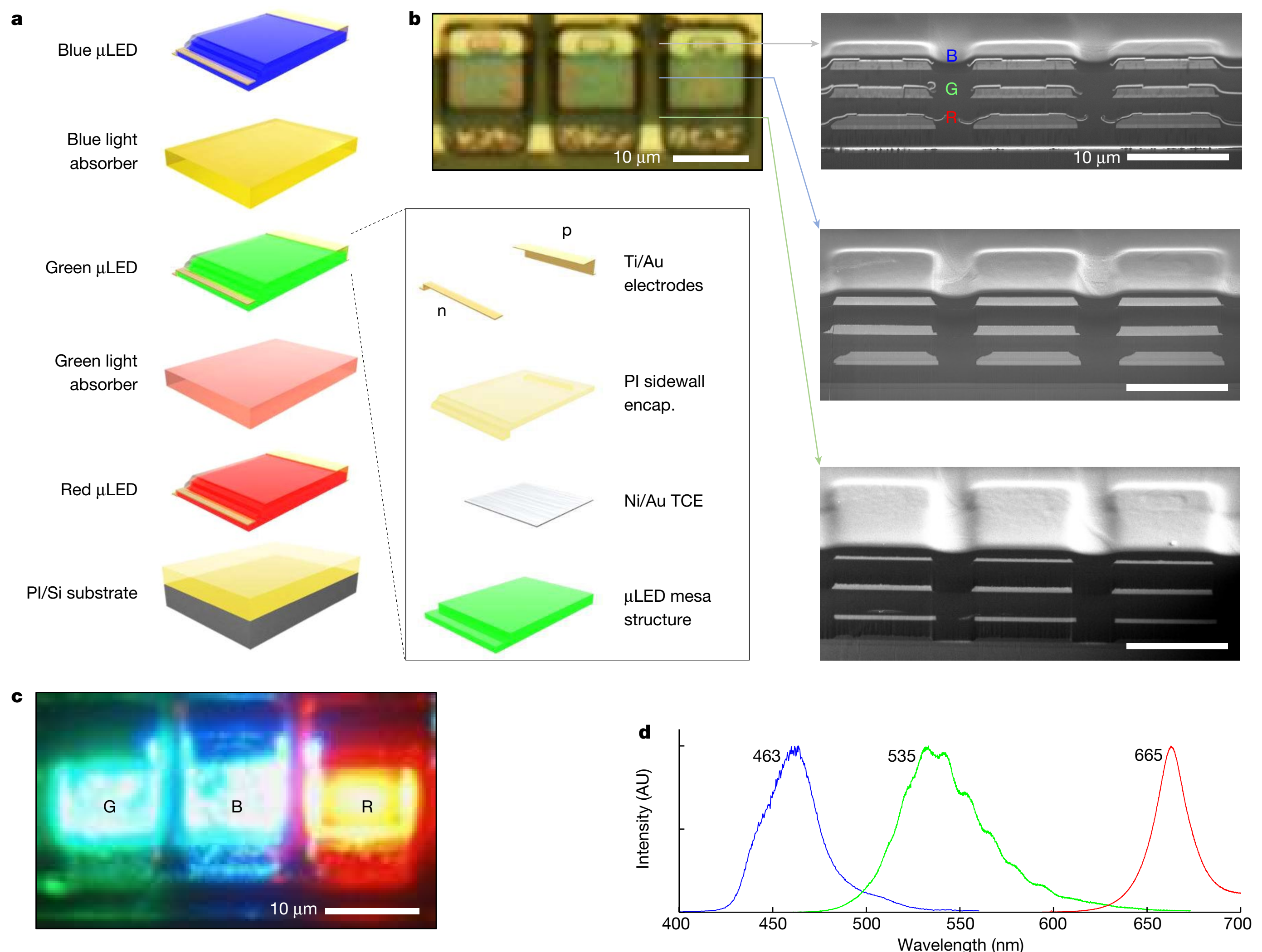

Fig. 1 | Vertically stacked, full-colour µLEDs enabled by 2DLT. a, Exploded schematic illustration of a vertical µLED pixel, consisting of RGB µLEDs and green and blue light-absorbing PI interlayers. Inset, exploded schematic illustration of a µLED consisting of µLED mesa structure, Ni/Au TCE, PI sidewall encapsulation layer and Ti/Au metal electrodes. **b**, Optical microscope image of three vertical µLED pixels side by side. Insets, cross-sectional SEM images of the device across p-contact (top), mesa (middle) and n-contact layer regions (bottom). **c**, EL image of vertical µLED device in **b** emitting three different colours in the dark. **d**, Normalized EL spectra of RGB µLEDs with peak wavelength of 665, 535 and 463 nm, respectively.

releasable and low-cost, to further advance vertical µLED microdisplay technology.

Here we demonstrate full-colour, vertically stacked µLEDs that achieve the smallest size (4 µm) and highest array density (5,100 pixels per inch (PPI)) reported to date, to our knowledge. This is enabled by two-dimensional materials-based layer transfer (2DLT) techniques[15–18] that allow (1) epitaxy of ultrathin RGB LEDs (thickness: 1–2 µm) on 2D material-coated substrates via either remote epitaxy or van der Waals epitaxy, (2) mechanical release of LED layers from 2D materials and subsequent reuse of the substrate, (3) stacking via the use of adhesive polymer layers and (4) top-down fabrication to yield vertical RGB µLEDs. Our vertical µLEDs achieve a total thickness of around 9 µm, which enables the fabrication of µLED arrays with record high density. Fast and precise mechanical release of LEDs from 2D materials allows high-throughput production of µLEDs, and reusability of the wafer reduces material cost. We also developed wavelength-selective polyimide (PI) absorbers (approximately 1.6 µm) that can serve as both adhesive interlayers and optical filters, preventing interference between LED membranes and eliminating the need to incorporate additional optical elements. We show a small µLED display with a pixel pitch of 14 µm (roughly 1,800 PPI) consisting of blue µLEDs integrated vertically with silicon thin-film transistors (TFTs) for active matrix operation. Last, we show the utility of 2DLT in the construction of large-scale µLED displays via high-resolution, selective mass transfer of µLEDs fabricated on 2D materials.

Figure 1a shows the overall architecture of vertically stacked µLEDs (see Extended Data Fig. 1 for process flow). We performed remote epitaxy of an AlGaAs-based red LED on a graphene-coated GaAs wafer, and van der Waals epitaxy of InGaN-based green and blue LEDs on hBN-coated sapphire substrates, which yielded single-crystalline RGB LED layers of thickness 1–2 µm. These were released from their substrates via the 2DLT process. The released LED membranes were stacked using PI absorber-bonding layers in the ascending order of bandgap energy, to minimize the absorption of light in the upward direction (pointing towards the viewer). µLEDs fabricated on the transferred membranes consist of transparent conductive electrodes (TCEs), mesa structures, a sidewall encapsulation layer (about 300 nm) and sputtered contact metals (Fig. 1a, inset; see Methods for detailed procedures).

To fabricate sub-10 µm vertical µLEDs, which are crucial for fully immersive AR/VR microdisplays, total µLED height must be minimized to reduce the aspect ratio and prevent errors during photolithography.

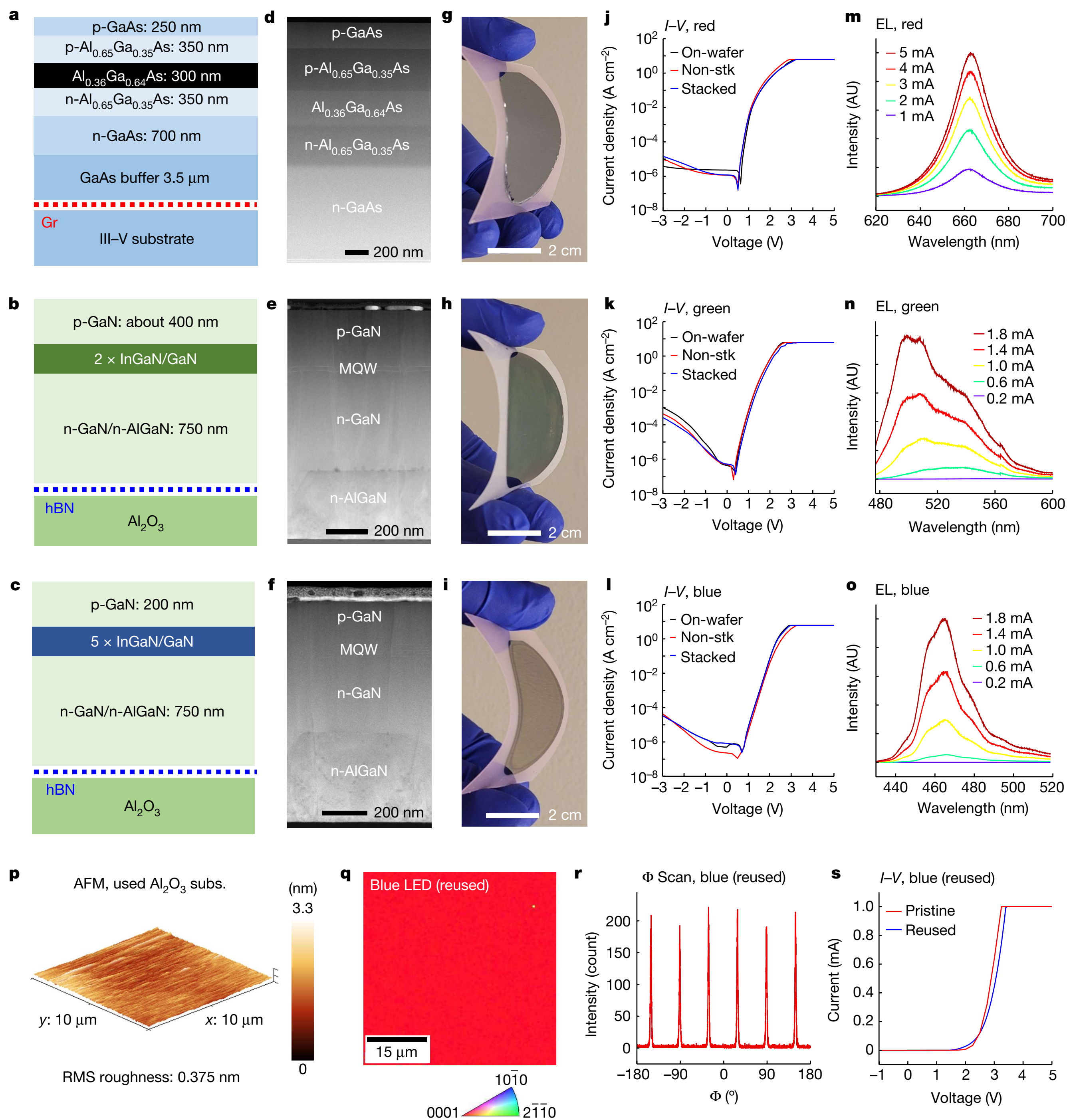

Fig. 2 | Ultrathin RGB LED membranes produced via 2DLT. a–c, Schematic illustrations of the epitaxial structures of an AlGaAs-based red LED grown on graphene-coated GaAs wafer (**a**) and InGaN-based green (**b**) and blue (**c**) LEDs grown on hBN-coated sapphire substrates. **d–f**, Cross-sectional STEM images of red (**d**), green (**e**) and blue (**f**) LEDs. **g–i**, Photographs of 2-inch-wafer-sized freestanding red (**g**), green (**h**) and blue (**i**) LED films on TRT. **j–l**, *I–V* curves of red (**j**), green (**k**) and blue (**l**) μLEDs fabricated on respective epitaxial wafers (on-wafer, black), on Si wafers following layer transfer (non-stacked (non-stk), red) and on Si wafers following vertical stacking (stacked, blue). **m–o**, Normalized EL spectra obtained from red (**m**), green (**n**) and blue (**o**) μLEDs fabricated on Si substrates under varying levels of injection current. **p**, AFM morphology image of a used sapphire substrate after removal of residual hBN layer. **q**,**r**, EBSD map (**q**) and XRD Φ scan data (**r**) obtained from blue LED grown on reused sapphire substrate. **s**, *I–V* curves obtained from blue LED devices grown on pristine (red) and reused (blue) sapphire substrates.

However, it has proved extremely challenging to reduce the thickness of vertical μLEDs due to inherent challenges in growing and handling freestanding LED films of near-submicron thickness, and also in regard to bonding and prevention of cross-talk between LEDs. The use of 2DLT enables the preparation of ultrathin, single-crystalline LEDs due to the relaxation of epitaxial strain on slippery 2D surfaces[22,24–28]. The addition of wavelength-selective dyes into the PI adhesion layer eliminates the need to introduce optical filters to prevent interference between LEDs. These modifications yield full-colour vertical μLEDs at a height of around 9 μm and sub-10 μm size (see Fig. 1b for optical and cross-sectional scanning electron microscopy (SEM) micrographs and Supplementary Fig. 1 for energy-dispersive X-ray (EDX) elemental maps

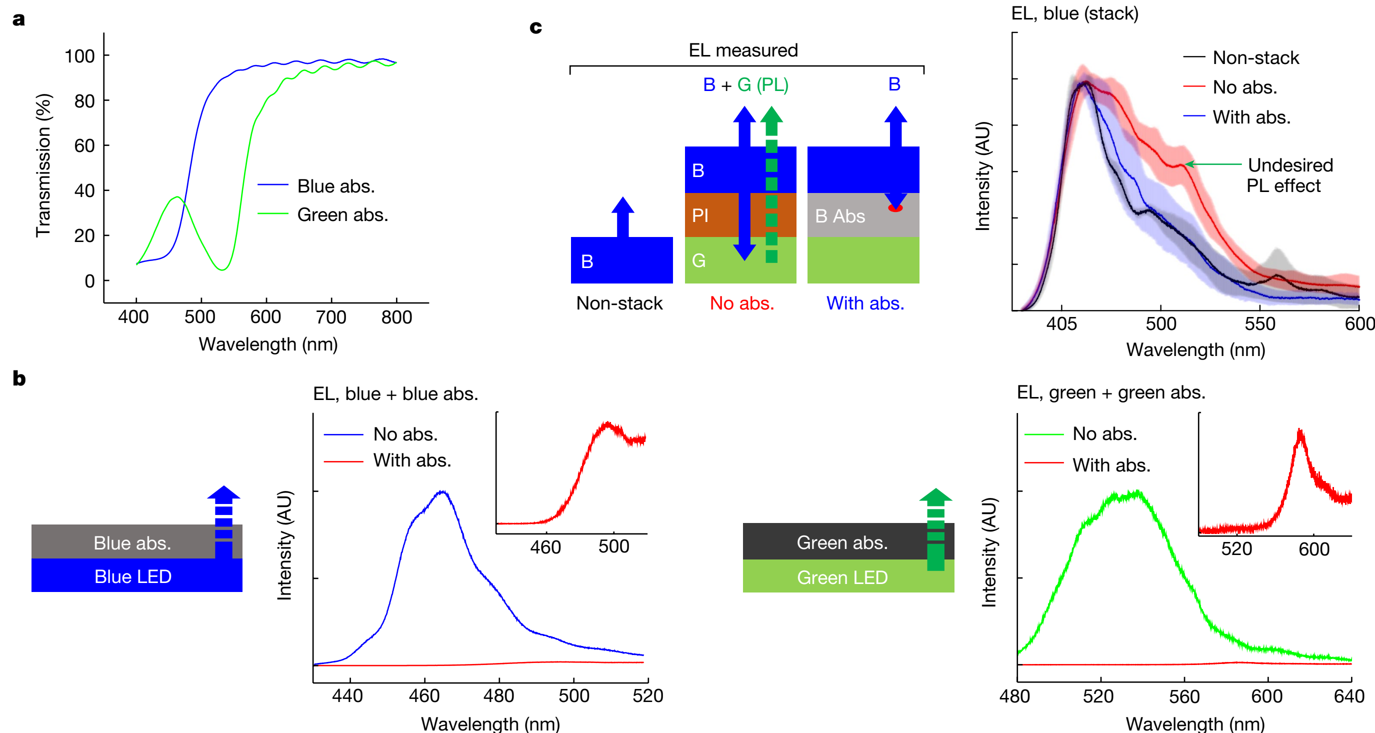

Fig. 3 | Prevention of PL via wavelength-specific, PI-based absorbers. **a**, Optical transmission spectra of blue and green light absorber layers preventing colour modulation due to cross-talk between LED layers. **b**, Schematic illustrations and normalized EL spectra of blue (left) and green (right) µLEDs coated with (with abs.) or without (no abs.) absorber layers, respectively. Insets, magnified plots of EL spectra of absorber-coated µLEDs. **c**, Schematic illustrations (left) and recorded EL spectra (right) of a transferred, non-stacked blue µLED (non-stack, black), a blue µLED integrated on top of a green µLED via a PI adhesive layer (no abs., red) and a blue µLED integrated on a green µLED via a blue absorber layer (with abs., blue). Error bars represent s.d. for at least three measurements.

illustrating stack composition). Figure 1c shows an electroluminescence (EL) microscopy image of three vertical µLEDs in parallel emitting different colours (see Supplementary Fig. 2 for details on the arrangement of metal contacts). EL spectra of RGB µLEDs (Fig. 1d) indicate peak wavelengths of 665, 535 and 463 nm, respectively.

Schematic illustrations (Fig. 2a–c) and cross-sectional scanning transmission electron microscopy (STEM; Fig. 2d–f) images illustrate the epitaxial structures of AlGaAs-based red LED on a graphene-coated GaAs wafer and InGaN-based green/blue LEDs on hBN-coated sapphire wafers. The thickness of RGB LED films is 1.9, 1.1 and 1.0 µm, respectively. The LEDs retain single-crystallinity and smooth surface morphology, as shown by electron backscatter diffraction (EBSD), X-ray diffraction (XRD) and atomic force microscopy (AFM) measurement results (Extended Data Fig. 2 and Supplementary Note 1). STEM images of the hBN–substrate interface and active regions for blue and green LEDs confirm the formation of an ultrasmooth hBN layer and multiquantum wells (MQWs), respectively, with EDX elemental maps confirming Al and In levels within the LED (Supplementary Fig. 3). LEDs grown on 2D materials can be peeled off readily using metal stressors and thermal release tapes (TRTs) due to their weak interaction with the substrate, as illustrated in Supplementary Video 1 and photographs of exfoliated 2-inch-wafer-sized RGB LED membranes (Fig. 2g–i and Supplementary Note 2). Mechanical robustness provided by the metal stressor allows transfer and stacking of freestanding LED layers without damage. As a result, the *I*–*V* characteristics and turn-on voltages of RGB µLEDs fabricated on their respective epitaxial wafers (Fig. 2j–l, black) are comparable to those of µLEDs fabricated from transferred (red) and vertically stacked (blue) membranes. In Supplementary Fig. 4a,b, the photograph of exfoliated 2-inch-wafer-scale blue LED film with no sign of physical damage indicates the high yield of the exfoliation process, with the optical microscope image and collective *I*–*V* curves of blue µLEDs (198 of 200 functional devices) illustrating the high yield of layer transfer and fabrication processes. Supplementary Fig. 4c shows the near-Lambertian radiation patterns of vertically stacked RGB µLEDs. Luminance of RGB µLEDs is in the range 10^4–10^6 cd m^{-2}, which is sufficient for AR/VR display applications[1] (see Extended Data Fig. 3 for measurements of luminance and efficiency and Supplementary Note 3 for discussion). For blue and green µLEDs, the TCE helps spread current on the less conductive p-GaN layer (Supplementary Fig. 5). Figure 2m–o shows the EL spectra of transferred RGB µLEDs under varying levels of injection current. The blueshift of peak wavelength for green LED emissions with increasing current is due to the quantum-confined Stark effect, which is commonly observed for InGaN-based LEDs[29].

A highly intriguing feature of 2DLT is the reusability of costly epitaxial wafers, which allows substantial reduction in µLED manufacturing cost. Unlike conventional lift-off techniques that require chemical-mechanical polishing to recover an epi-ready surface[30–32], precisely defined crack propagation through 2D material in 2DLT ensures that the substrate remains undamaged through the exfoliation process and can be recycled after removal of the residual 2D layer (Supplementary Note 4). A simple dry transfer process completely peels off the hBN layer from a used sapphire substrate, as indicated by the disappearance of B 1s and N 1s peaks in the X-ray photoelectron spectroscopy (XPS) spectra shown in Extended Data Fig. 4a (Methods). AFM analysis shows RMS roughness of 0.375 nm for the substrate after hBN removal (Fig. 2p). We subsequently grew hBN and blue LED on the wafer and performed EBSD analysis (Fig. 2q), XRD Φ scan (Fig. 2r) and *I*–*V* curve measurement on fabricated µLEDs (Fig. 2s). EBSD and XRD data indicate that the blue LED grown on reused sapphire substrate is entirely single-crystalline (0001) without in-plane rotations, and its *I*–*V* curve (blue) appears comparable to that of blue LED grown on pristine (red) sapphire substrate. SEM images of LEDs grown on pristine and

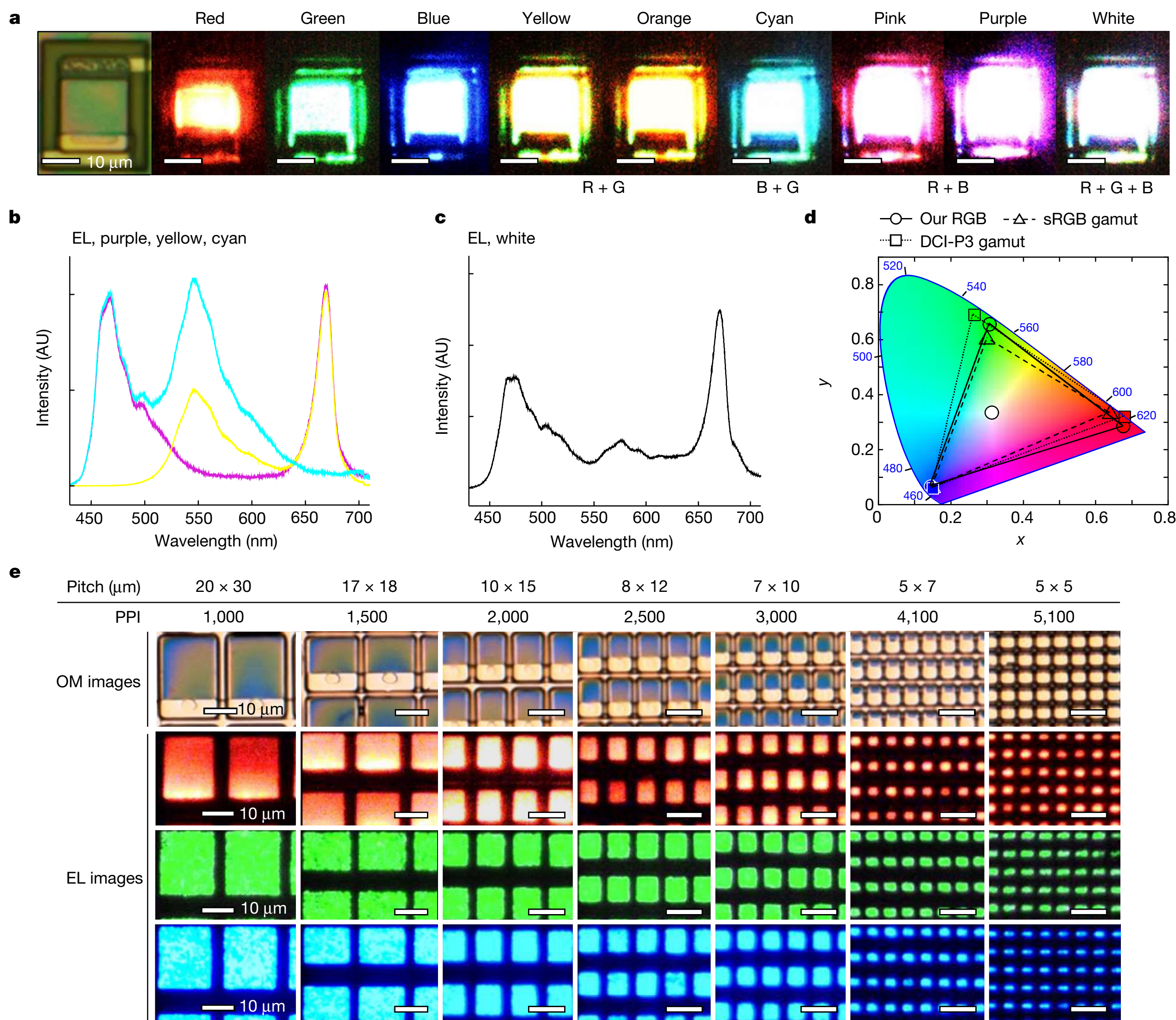

Fig. 4 | 2DLT-enabled full-colour vertical ultrasmall μLEDs. a, EL microscopy images of vertical μLEDs illuminating red, green, blue, yellow, orange, cyan, pink, purple and white light via mixing of RGB colours. **b**, Representative EL spectra of purple, yellow and cyan light emitted by vertical μLEDs. **c**, Representative EL spectrum of white light emitted by vertical μLEDs. **d**, Chromaticity of vertical μLEDs (solid line and circle) in the CIE 1931 colour space, plotted along with sRGB (dotted line and triangle) and DCI-P3 (dotted line and square) colour gamuts. The position of the white EL in **c** is indicated by a white circle at coordinates (0.314, 0.341). **e**, Optical and EL microscopy images of vertical μLED arrays for near-eye display applications, with seven different sizes (PPI 1,000–5,100).

reused wafers show comparable surface morphology (Extended Data Fig. 4c,d). These results strongly support the reusability of sapphire substrates following 2DLT. Epitaxial wafers used in remote epitaxy are also found to be reusable[33].

An important consideration in the design of vertically stacked, full-colour μLEDs is the prevention of interference between LED layers by absorption and re-emission, a phenomenon known as photoluminescence (PL)[8]. Downward emissions from blue and green LEDs can induce PL in adjacent green and red LEDs, respectively, making them turn on simultaneously and introduce unwanted colour modulation. To prevent this, we conceived PI-based blue and green optical absorbers and inserted them as adhesive interlayers between G/B and R/G LEDs, respectively, to block downward emissions (see Methods for detailed procedures and Extended Data Fig. 5 for data on absorber optimization). Blue and green absorbers are designed to strongly absorb blue (approximately 460 nm) and green light (approximately 540 nm), respectively, as indicated by the optical transmission spectra shown in Fig. 3a. As coatings on LEDs they can completely quench respective target colour emissions while transmitting over 90% of non-target colour emissions, as confirmed by schematic illustrations and EL spectra in Fig. 3b and Supplementary Fig. 6, respectively. Most importantly, evidence of their effectiveness in preventing PL in the vertical stack configuration is shown in Fig. 3c and Supplementary Fig. 7. Whereas green PL is observed in the EL spectra of a blue LED stacked on a green LED by a PI layer, it is absent in the EL spectra of a device containing a blue absorber layer. These PI-based absorber-bonding layers play a critical role in reducing the combined thickness of vertical μLEDs.

The precise vertical overlap of RGB emission regions and the small thickness of vertical μLEDs enable natural and high-resolution colour mixing. EL microscopy images (Fig. 4a and Supplementary Video 2) illustrate homogeneous illumination of yellow, orange, cyan, pink, purple and white light by vertical μLEDs. Representative EL spectra of

purple, yellow, cyan and white emissions are shown in Fig. 4b,c. Figure 4d shows the chromaticity of vertical μLEDs in the CIE 1932 colour space, along with standard RGB (sRGB) and DCI-P3 colour gamuts. The colour space achieved by our μLEDs has 99.4 and 86.9% overlap with sRGB and DCI-P3, respectively, indicating the potential to cover the full range of colours required for display applications. The CIE colour coordinates for RGB LEDs are (0.676, 0.285), (0.307, 0.656) and (0.145, 0.066), respectively, and RGB colour purities are 88.3, 90.5 and 94.1%, respectively (see Supplementary Note 5 for calculation). A white circle at (0.314, 0.341) denotes the position of the white EL shown in Fig. 4c.

The greatest strength of our vertical μLED technology is the potential to substantially reduce the size and pitch of RGB μLEDs compared with traditional displays featuring lateral subpixel layouts. To demonstrate this, we fabricated arrays of vertical μLEDs with pitch (excluding backplane) ranging from 20 × 30 μm^2 (around 1,000 PPI) down to 5 × 5 μm^2 (around 5,100 PPI), as shown in the microscopy images in Fig. 4e and Supplementary Fig. 8. To our knowledge, only Ostendo Technologies Inc. has reported sub-10 μm full-colour μLED displays[13,14], with other reports of 1,000+ PPI μLED displays being limited to either monochrome displays[34–36] or full-colour displays based on colour conversion layers that compromise emission efficiency[37,38]. The μLED array density achieved in this study is more than one order of magnitude higher than the PPIs of self-emitting RGB μLED displays reported in the literature (Extended Data Table 1) and in news articles (Supplementary Table 1). The range of μLED densities achieved by our technology will be sufficient to meet the exceptional demands of human vision for near-eye display[2,21].

A key element of functional displays is the capability to address individual LEDs via active matrix operation. To demonstrate this, we fabricated 300-nm-thick silicon membrane TFTs on a silicon-on-insulator wafer, which was integrated vertically with blue μLEDs obtained via van der Waals epitaxy. Extended Data Fig. 6 shows a 30 × 30 array of Si TFTs with dimensions 2.2 μm × 9.2 μm × 300 nm, channel width/length 1.5/2.2 μm, on-off ratio of 10^5 and current saturation at different gate voltages. Layer transfer and fabrication of blue μLEDs on top of Si TFTs, followed by electrical interconnection of each μLED with a TFT, yielded an active matrix μLED display with pixel pitch of 14 μm (about 1,800 PPI; Extended Data Fig. 7a–c and Methods). Individual μLEDs can be addressed by applying current to the p-contact of LED (V_{SS}) while applying voltage to the gate to activate the TFT (scan line), enabling display of the 'mit' logo (Extended Data Fig. 7d). To construct a full-colour μLED active matrix display, silicon membranes may be similarly transferred[39] and stacked to form vertical TFTs that can be integrated with vertical μLEDs, as outlined in Supplementary Fig. 9. Such an integration scheme could maximize the pixel density of μLED displays to potentially achieve the long-awaited fully immersive AR/VR displays.

Although AR/VR microdisplays are intriguing applications for μLEDs, display manufacturers have greater financial motivations towards μLED-based flat-panel displays for televisions, smartphones and other consumer electronics. Contrary to microdisplays, flat-panel displays require lower pixel density (100–500 PPI) and a larger display area (up to 80 inches and beyond), making mass transfer the desired approach (see Supplementary Fig. 10a for illustration of process flow)[3,5]. Currently the major cost driver for these technologies is insufficient transfer yield, in particular for smaller μLEDs[3,4]. We conceived a solution using 2DLT-based mass transfer of stacked μLED chips. Extended Data Fig. 8 illustrates the selective transfer of blue LEDs (size: 10 μm) on a hBN-coated sapphire substrate using partially developed photoresist patterns, Ni stressors and TRTs, which enables facile yet highly resolved extraction of μLED chips among a densely packed array (chip-to-chip separation about 10 μm; Methods). Such a process can reduce the number of transfer events by a factor of three, thereby increasing both manufacturing yield and speed, as illustrated in Supplementary Fig. 10b. Mass transfer of isolated vertical μLED chips (Supplementary Fig. 11) could expand the utility of vertical μLED technology to large-scale, flat-panel displays, establishing the overarching potential impact of 2DLT in the field.

In summary, we have demonstrated the strategies for 2D material-based epitaxy, layer transfer and heterogeneous integration of ultrathin, single-crystalline RGB LED films in the construction of vertically stacked, full-colour μLED arrays with record high device density. We have also demonstrated an active matrix display based on blue μLEDs integrated vertically with Si TFTs, as well as a 2DLT-based mass transfer process that could extend the utility of vertical μLEDs to large-scale displays. The performance of vertical μLEDs could be further improved by the development of remote epitaxy-based blue and green LEDs with enhanced material and device characteristics (Extended Data Fig. 9 and Supplementary Note 6), transparent conductive oxides with higher transparency and distributed Bragg reflectors combined with colourless adhesion layers that could eliminate the loss of downward LED emissions. The materials, device architectures and fabrication processes presented here have the potential to help realize full-colour, μLED-based AR/VR microdisplays, televisions and smartphone displays, as well as broad classes of three-dimensional integrated photonic, electronic and optoelectronic systems.

Online content

Any methods, additional references, Nature Portfolio reporting summaries, source data, extended data, supplementary information, acknowledgements, peer review information; details of author contributions and competing interests; and statements of data and code availability are available at https://doi.org/10.1038/s41586-022-05612-1.

1. Lee, V. W., Twu, N. & Kymissis, I. Micro-LED technologies and applications. *Inf. Disp.* **32**, 16–23 (2016).
2. Zhan, T., Yin, K., Xiong, J., He, Z. & Wu, S.-T. Augmented reality and virtual reality displays: perspectives and challenges. *iScience* **23**, 101397 (2020).
3. Gong, Z. Layer-scale and chip-scale transfer techniques for functional devices and systems: a review. *Nanomaterials (Basel)* **11**, 842 (2021).
4. Wu, Y., Ma, J., Su, P., Zhang, L. & Xia, B. Full-color realization of micro-LED displays. *Nanomaterials (Basel)* **10**, 2482 (2020).
5. Marinov, V. R. 52-4: Laser-enabled extremely-high rate technology for μLED assembly. *SID Symp. Dig. Tech. Pap.* **49**, 692–695 (2018).
6. Bower, C. A. et al. Emissive displays with transfer-printed assemblies of 8 μm x 15 μm inorganic light-emitting diodes. *Photon. Res.* **5**, A23–A29 (2017).
7. Chun, J. et al. Vertically stacked color tunable light-emitting diodes fabricated using wafer bonding and transfer printing. *ACS Appl. Mater. Interfaces* **6**, 19482–19487 (2014).
8. Kang, C.-M. et al. Monolithic integration of AlGaInP-based red and InGaN-based green LEDs via adhesive bonding for multicolor emission. *Sci. Rep.* **7**, 10333 (2017).
9. Kang, C.-M. et al. Hybrid full-color inorganic light-emitting diodes integrated on a single wafer using selective area growth and adhesive bonding. *ACS Photonics* **5**, 4413–4422 (2018).
10. Jin, H. et al. Vertically stacked RGB LEDs with optimized distributed Bragg reflectors. *Opt. Lett.* **45**, 6671–6674 (2020).
11. Li, L. et al. Transfer-printed, tandem microscale light-emitting diodes for full-color displays. *Proc. Natl Acad. Sci. USA* **118**, e2023436118 (2021).
12. Mun, S.-H. et al. Highly efficient full-color inorganic LEDs on a single wafer by using multiple adhesive bonding. *Adv. Mater. Interfaces* **8**, 2100300 (2021).
13. El-Ghoroury, H. S., Chuang, C.-L. & Alpaslan, Z. Y. 26.1: Invited paper: quantum photonic imager (QPI): a novel display technology that enables more than 3D applications. *SID Symp. Dig. Tech. Pap.* **46**, 371–374 (2015).
14. Yadavalli, K., Chuang, C.-L. & El-Ghoroury, H. Monolithic and heterogeneous integration of RGB micro-LED arrays with pixel-level optics array and CMOS image processor to enable small form-factor display applications. In *Proc. SPIE 11310, Optical Architectures for Displays and Sensing in Augmented, Virtual, and Mixed Reality (AR, VR, MR)* (eds Kress, B. C. & Peroz, C.) 113100Z (SPIE, 2020).
15. Ayari, T. et al. Wafer-scale controlled exfoliation of metal organic vapor phase epitaxy grown InGaN/GaN multi quantum well structures using low-tack two-dimensional layered h-BN. *Appl. Phys. Lett.* **108**, 171106 (2016).
16. Li, X. et al. Large-area two-dimensional layered hexagonal boron nitride grown on sapphire by metalorganic vapor phase epitaxy. *Crystal Growth Des.* **16**, 3409–3415 (2016).
17. Kim, Y. et al. Remote epitaxy through graphene enables two-dimensional material-based layer transfer. *Nature* **544**, 340–343 (2017).
18. Kim, H. et al. Impact of 2D–3D heterointerface on remote epitaxial interaction through graphene. *ACS Nano* **15**, 10587–10596 (2021).
19. Kim, H.-s et al. Unusual strategies for using indium gallium nitride grown on silicon (111) for solid-state lighting. *Proc. Natl Acad. Sci. USA* **108**, 10072–10077 (2011).
20. Kim, T.-i et al. High-efficiency, microscale GaN light-emitting diodes and their thermal properties on unusual substrates. *Small* **8**, 1643–1649 (2012).

21. LaValle, S. M. *Virtual Reality* (Cambridge Univ. Press, 2016).
22. Kum, H. et al. Epitaxial growth and layer-transfer techniques for heterogeneous integration of materials for electronic and photonic devices. *Nat. Electron.* **2**, 439–450 (2019).
23. Cheng, J.-H., Wu, Y. S., Peng, W. C. & Ouyang, H. Effects of laser sources on damage mechanisms and reverse-bias leakages of laser lift-off GaN-based LEDs. *J. Electrochem. Soc.* **156**, H640 (2009).
24. Jiang, J. et al. Carrier lifetime enhancement in halide perovskite via remote epitaxy. *Nat. Commun.* **10**, 4145 (2019).
25. Journot, T. et al. Remote epitaxy using graphene enables growth of stress-free GaN. *Nanotechnology* **30**, 505603 (2019).
26. Bae, S.-H. et al. Graphene-assisted spontaneous relaxation towards dislocation-free heteroepitaxy. *Nat. Nanotechnol.* **15**, 272–276 (2020).
27. Chang, H. et al. Graphene-driving strain engineering to enable strain-free epitaxy of AlN film for deep ultraviolet light-emitting diode. *Light Sci. Appl.* **11**, 88 (2022).
28. Chen, Z. et al. Improved epitaxy of AlN film for deep-ultraviolet light-emitting diodes enabled by graphene. *Adv. Mater.* **31**, 1807345 (2019).
29. Ryou, J. et al. Control of quantum-confined Stark effect in InGaN-based quantum wells. *IEEE J. Sel. Top. Quantum Electron.* **15**, 1080–1091 (2009).
30. Chen, J. & Packard, C. E. Controlled spalling-based mechanical substrate exfoliation for III-V solar cells: a review. *Sol. Energy Mater. Sol. Cells* **225**, 111018 (2021).
31. Zhang, B., Luo, C. & Li, Y.-F. Damage-free transfer of GaN-based light-emitting devices and reuse of sapphire substrate. *ECS J. Solid State Sci. Technol.* **9**, 065019 (2020).
32. Bauhuis, G. J. et al. Wafer reuse for repeated growth of III–V solar cells. *Prog. Photovolt.* **18**, 155–159 (2010).
33. Kim, H. et al. Multiplication of freestanding semiconductor membranes from a single wafer by advanced remote epitaxy. Preprint at https://arxiv.org/abs/2204.08002 (2022).
34. Day, J. et al. III-nitride full-scale high-resolution microdisplays. *Appl. Phys. Lett.* **99**, 031116 (2011).
35. Meng, W. et al. Three-dimensional monolithic micro-LED display driven by atomically thin transistor matrix. *Nat. Nanotechnol.* **16**, 1231–1236 (2021).
36. Ludovic, D. et al. Processing and characterization of high resolution GaN/InGaN LED arrays at 10 micron pitch for micro display applications. In *Proc. SPIE 10104, Gallium Nitride Materials and Devices XII* (eds Chyi, J.-I. et al.) 1010422 (SPIE, 2017).
37. Chen, G.-S., Wei, B.-Y., Lee, C.-T. & Lee, H. Y. Monolithic red/green/blue micro-LEDs with HBR and DBR structures. *IEEE Photonics Technol. Lett.* **30**, 262–265 (2018).
38. Park, J. et al. Electrically driven mid-submicrometre pixelation of InGaN micro-light-emitting diode displays for augmented-reality glasses. *Nat. Photon.* **15**, 449–455 (2021).
39. Carlson, A., Bowen, A. M., Huang, Y., Nuzzo, R. G. & Rogers, J. A. Transfer printing techniques for materials assembly and micro/nanodevice fabrication. *Adv. Mater.* **24**, 5284–5318 (2012).

Publisher's note Springer Nature remains neutral with regard to jurisdictional claims in published maps and institutional affiliations.

Springer Nature or its licensor (e.g. a society or other partner) holds exclusive rights to this article under a publishing agreement with the author(s) or other rightsholder(s); author self-archiving of the accepted manuscript version of this article is solely governed by the terms of such publishing agreement and applicable law.

© The Author(s), under exclusive licence to Springer Nature Limited 2023

Methods

2DLT of red, green and blue LEDs

Epitaxy of red AlGaAs LED on graphene-coated GaAs substrate. A metal-organic chemical vapour deposition (MOCVD) reactor with a close-coupled showerhead design was used to grow red AlGaAs LEDs, with nitrogen as carrier gas. Trimethyl-gallium, trimethyl-aluminium and arsine served as precursors for Ga, Al and As, respectively, and dimethyl-zinc and disilane served as Zn and Si precursors for p- and n-doping of active layers, respectively. The pressure level for all growths was 100 Torr. The epitaxy process began with growth of a thin GaAs nucleation layer on the graphene-coated substrate at 475 °C, followed by the full buffer at 650 °C at a growth rate of around 33 nm min^{-1}. The active layers were grown in the sequence n-GaAs bottom contact layer (700 nm), n-$Al_{0.65}Ga_{0.35}As$ lower barrier (350 nm), $Al_{0.36}Ga_{0.64}As$ emitter layer (300 nm), p-$Al_{0.65}Ga_{0.35}As$ upper barrier (350 nm) and p-GaAs top contact layer (250 nm), all at 700 °C and a growth rate of about 33 nm min^{-1}. Cooling down the reactor with arsine flow prevented surface desorption.

Epitaxy of blue InGaN LED on hBN-coated sapphire substrate. An Aixtron 3 × 2-inch wafer, close-coupled showerhead reactor system grew the hBN layer and blue InGaN LED on an Al_2O_3 (0001) substrate via metal-organic vapour-phase epitaxy (MOVPE). Triethyl-boron, trimethyl-gallium/triethyl-gallium, trimethyl-indium, trimethyl-aluminium and ammonia served as precursors for B, Ga, In, Al and N, respectively, and silane and bis(cyclopentadienyl)magnesium served as Si and Mg precursors for n- and p-doping of active layers, respectively. Epitaxy began with growth of the hBN layer (approximately 3 nm) at 1,300 °C, followed by the n-AlGaN layer (approximately 250 nm; Al mole fraction around 14 ± 2%) at 1,100 °C. The growth sequence for active layers included an n-GaN bottom contact layer (500 nm), five periods of InGaN quantum well layer (2.5 nm; In mole fraction around 15 ± 1%) and GaN barrier layer (12 nm), and a p-GaN top contact layer (170 nm). Electron and hole carrier concentrations in Si- and Mg-doped GaN layers were 5×10^{18} and 1×10^{1} cm^{-3}, respectively.

Epitaxy of green InGaN LED on hBN-coated sapphire substrate. The MOCVD system was used to grow InGaN/GaN MQWs and a p-GaN layer for green emission on top of an n-GaN/n-AlGaN/hBN/Al_2O_3 (0001) substrate, prepared via the process described in the previous paragraph for blue LEDs, using high-purity hydrogen (H_2) or nitrogen (N_2) as carrier gas. Trimethyl-gallium, trimethyl-indium and ammonia served as precursors for Ga, In and N, respectively, with bis(cyclopentadienyl) magnesium as Mg precursor for doping of the p-GaN layer. Epitaxy began with the growth of MQWs consisting of two periods of the InGaN quantum well (2.3 nm) and GaN barrier layers (21 nm) at 710 °C, with growth rates of 0.22 Å s^{-1} for InGaN QW and 1.17 Å s^{-1} for the GaN barrier. NH_3-rich ambient prevented thermal decomposition of the n-GaN layer during temperature ramp-up. Growth temperature for the p-GaN top contact layer (200 nm) was 1,000 °C. Rapid thermal annealing (RTA) at 800 °C for 5 min in N_2 ambient activated the Mg dopant in the p-GaN layer.

Remote epitaxy of blue InGaN LED on GaN substrate. Both molecular beam epitaxy (MBE) and MOCVD were used to grow an InGaN-based blue LED via remote epitaxy. In an MBE chamber boron nitride (BN) was grown on a GaN (0001) wafer at 760 °C, after which a 300-nm-thick GaN buffer was grown at 820 °C in situ. Elemental boron and gallium, in effusion cells, and nitrogen plasma served as precursors for B, Ga and N. The substrate was then transferred to an MOCVD chamber in which the active layers for blue emission were grown in the order n-GaN bottom contact layer (400 nm), five periods of InGaN quantum well (2.3 nm) and GaN quantum barrier (21 nm), and p-GaN top contact layer (200 nm). High-purity hydrogen (H_2) or nitrogen (N_2) was used as carrier gas. Trimethyl-gallium, trimethyl-indium and ammonia served as precursors for Ga, In and N, respectively, and silane and bis(cyclopentadienyl) magnesium as Si and Mg precursors for n- and p-type doping of GaN, respectively. RTA at 800 °C for 5 min in N_2 ambient activated Mg dopant in the p-GaN layer.

2DLT. For red LEDs, electron-beam (e-beam) evaporation of Ti (30 nm) followed by sputtering of a tensile-strained Ni stressor layer (4 µm) via DC sputtering, attachment of a TRT (release temperature: 120 °C; Revalpha, Semiconductor Equipment Corp.) and gradual release of the tape exfoliated the LED film at the LED–graphene interface. Reactive ion etching (RIE; PlasmaPro 100 Cobra 300 System, Oxford Instruments) using Cl_2 gas etched away the GaAs buffer under the device layers. For green and blue LEDs, e-beam evaporation of Ni/Au (10/10 nm) followed by RTA in air at 450 °C for 3 min formed TCEs. Oxygen plasma treatment for 1 min, DC sputtering of Al (3 µm), attachment of TRT and removal of the tape exfoliated the LEDs. The choice of Al as a support layer was based on the high etch selectivity of Al etchant type D (Transene Company Inc.) for Al over Ni/Au TCE.

Heterogeneous integration of full-colour vertical µLEDs

Adhesive bonding of red AlGaAs LED on receiver substrate. Plasma-enhanced chemical vapour deposition (PECVD) of SiO_2 (500 nm; STS PECVD) on Si wafer (thickness: 380 µm; University Wafer), followed by photolithography, e-beam evaporation of Ti/Ni (15/150 nm) and lift-off, prepared the receiver substrate with align keys. Both the receiver substrate and red LED on TRT were treated with oxygen plasma (Anatech Barrel Plasma System), spin-coated with a 1 vol% aqueous solution of (3-aminopropyl)triethoxysilane (APTES, Sigma-Aldrich) at a speed of 3,000 rpm for 30 s and baked at 110 °C for 1 min. Receiver substrate was then spin-coated with PI precursor (PI-2545, HD Microsystems) at 3,000 rpm for 30 s, partially cured at 110 °C for 30 s, pressed against the LED film on TRT using a steel vice (Toolmaker's vise, Tormach, Inc.) and partially cured on a hot plate at 180 °C for 10 min. Thermal release of the TRT from substrate by heating at 150 °C, and full curing of the PI by pressing the sample in a vice and placing it in a convection oven at 250 °C for 1 h, completed the bonding process. Wet etching in $FeCl_3$ solution (MG Chemicals) and 5:1 buffered oxide etchant (BOE, J. T. Baker) removed Ti/Ni layers.

Fabrication of red AlGaAs µLEDs. Photolithography (AS200 i-line Stepper) and RIE using Cl_2 gas first defined mesa structures and then the outer boundary lines of µLEDs. Spin-coating a PI precursor diluted 1:1 by weight in 1-methyl-2-pyrrolidinone (NMP, Sigma-Aldrich) at a speed of 3,000 rpm for 30 s, followed by curing at temperatures of 110, 150 and 250 °C for 1, 3 and 60 min, respectively, formed a thin coating of PI (about 300 nm). Photolithography and RIE using O_2 gas partially exposed n- and p-type contact layers, and subsequent photolithography, DC sputtering of Ti/Au (15/150 nm; AJA Sputterer) and metal lift-off completed n- and p-type metal interconnections.

Preparation of PI absorber layers. Dissolving visible yellow dye powder (Epolight 5843, Epolin) in PI precursor to form a 0.5 wt% solution prepared the blue absorber precursor, and dissolving red visible absorbing dye (Epolight 5396, Epolin) in PI precursor to form a 1.0 wt% solution prepared the green absorber precursor. Spin-coating precursors on glass slides at a speed of 3,000 rpm for 30 s and curing at temperatures of 110, 150 and 250 °C for 1, 3 and 60 min, respectively, prepared PI absorber samples for ultraviolet-visible analysis (Extended Data Fig. 5).

Integration of green and blue LEDs and fabrication of vertical µLEDs. Procedures almost identical to those described above for layer transfer and fabrication of red µLEDs were used to integrate and fabricate green and blue LED layers on top of red µLEDs; differences

included the use of green and blue absorber precursors rather than PI precursor to transfer green and blue LED layers, respectively, and the use of Al etchant type D to remove Al support layers. After transfer and fabrication of all three LED layers, photolithography and RIE using O_2 gas removed parts of the blue and green absorber layers to expose metal contact pads for green and red LEDs. Photolithography, DC sputtering of Ti/Au (15/400 nm) and lift-off electrically connected the three n-contact metal pads for RGB LEDs. Photolithography, DC sputtering of Ti/Au (15/100 nm) and metal lift-off formed a black matrix for the samples shown in Fig. 4a.

Reuse of sapphire wafer for van der Waals epitaxy of blue InGaN LED

After exfoliation of the blue LED layer via 2DLT, e-beam evaporation and DC sputtering of Ni/Ni (20/1.5 μm), followed by attachment and peeling off of TRT, exfoliated the remaining hBN layer on used sapphire substrate. Placing of the wafer in $FeCl_3$ solution for 3 min removed residual Ni, preparing the wafer for additional growth processes.

Fabrication of Si TFT-integrated blue μLED array

Chemical-mechanical polishing reduced the total thickness of the silicon-on-insulator wafer (top Si 300 nm; buried SiO_2 1 μm; Si handle 400 μm) before device fabrication. PECVD deposition of a silicon oxide layer (300 nm) followed by photolithography and RIE using CF_4/O_2 gas defined the mask pattern for doping of source and drain contacts of the Si TFT. Solid-state diffusion of phosphorus at 900 °C, a drive-in process at 950 °C and a cleaning process using BOE and piranha solution completed the doping. Photolithography and RIE using SF_6 gas defined the shape of each TFT. Atomic layer deposition of Al_2O_3 (roughly 30 nm) on an oxygen plasma-treated sample formed the gate oxide, and subsequent photolithography and RIE using CF_4/O_2 gas exposed the source and drain contacts. Photolithography, sputtering of Ti/Au (15/130 nm) and metal lift-off formed the metal contact (for source) and V_{DD} lines. Spin-coating of a PI precursor diluted 1:1 by weight in NMP at 3,000 rpm for 30 s, followed by curing at temperatures of 110, 150 and 250 °C for 1, 3 and 60 min, respectively, formed a thin coating of PI (roughly 300 nm). Photolithography and RIE using O_2 gas exposed the gate and drain contacts and subsequent photolithography, sputtering of Ti/Au (15/130 nm) and metal lift-off formed the gate electrode and scan lines. The procedures described above for layer transfer and μLED fabrication were used to form an array of blue μLEDs on top of Si TFTs. Photolithography and RIE using O_2 gas formed via holes exposing the drain contacts of Si TFTs, and subsequent photolithography, sputtering of Ti/Au (15/130 nm) and metal lift-off formed electrical interconnections between the n-GaN contact of blue LEDs with the drain contact of Si TFTs, as well as with V_{SS} lines.

Device characterization

Spectroscopy equipped by the Renishaw Invia Reflex Micro Raman system collected EL spectra for LEDs. A 50× objective lens collected sample emissions, resolved using a 1,200 g mm^{-2} grating and a commercial silicon CCD detector. Probe station (Signatone Corp.), equipped with a semiconductor parameter analyser (Agilent 4156C, Keysight Technologies) and camera system (connected to an optical microscope for collection of images and videos), recorded the I–V curves of LEDs, transfer and output characteristics of Si TFTs, EL microscopy images and video recordings. A computer-controlled source measurement unit (Keithley 2636A) and a calibrated silicon photodiode (Thorlabs, no. FDS1010-CAL) recorded I–V characteristics and the photodiode response of each μLED which, combined with photodiode spectral responsivity and the emission spectrum of each LED, yielded the luminance and external quantum efficiency (EQE) of each μLED under forward bias[40]. Far-field radiation patterns for stacked μLEDs were measured by driving each μLED at a constant current of 1 mA and recording the photocurrent from a Si photodiode (Newport 818UV) positioned 12 cm away from the surface of the μLED. The photodiode was mounted on a manual goniometer, and the μLED was kept stationary at the goniometer's centre of rotation. The photodiode was rotated around the stacked μLEDs, scanning from −90° to +90° at a step size of 5°. A MultiLab 2000 XPS system (Thermo VG Scientific) using a Mg Kα source collected XPS spectra for hBN samples at room temperature. Peak energies were calibrated by the C 1 s peak at 284.8 eV. A Park Systems NX10 Atomic Force Microscope measured surface roughness using a non-contact mode. A UV/Vis/NIR spectrophotometer (Lambda 1050, PerkinElmer, Inc.) collected optical transmission spectra for blue and green light-absorbing layers and also for Ni/Au TCEs. A FEI Helios 660 Focused Ion Beam, with a final milling voltage of 5 keV, prepared cross-sectional specimens of vertical μLEDs. Deposition of C and Pt layers before milling prevented ion beam damage. Scanning electron microscopy–energy-dispersive X-ray spectroscopy elemental maps were taken using EDAX TEAM software. A Titan Themis Z G3 Cs-corrected microscope equipped with Velox software for drift-corrected frame imaging and EDX analysis collected STEM images and EDX elemental maps. The operating beam voltage was 200 kV in STEM mode. A ZEISS Merlin high-resolution SEM equipped with an EBSD detector collected EBSD data at 20 kV and 10 nA and a working distance of 15 mm. A Bruker D8 HRXRD equipped with a four-bounce Ge(022) incident beam monochromator, which eliminates all incident wavelengths except Cu Kα1 (λ = 1.540562 Å), collected XRD 2θ-ω and Φ scan data.

2DLT-based chip transfer

Photolithography and RIE using Cl_2 gas defined the blue μLEDs and hBN layer, exposing the sapphire substrate underneath. Photolithography via underexposure of ultraviolet light formed a photoresist pattern that exposed the upper bodies of selected μLED chips but not the sapphire substrate surrounding them. E-beam evaporation of Ti (40 nm) followed by DC sputtering of Ni (3.5 μm), followed by the attachment of TRT, enabled the exfoliation of selected μLED chips among the chip array. Dipping the sapphire substrate in remover PG (Kayaku Advanced Materials, Inc.) removed photoresist on the substrate, and RIE using O_2 gas removed photoresist residue on the exfoliated sample on TRT. Adhesive bonding procedures described above transferred selectively released μLEDs on TRT to a PECVD SiO_2-coated Si wafer. Chemical wet etching in both $FeCl_3$ and BOE removed Ti/Ni layers, and photolithography and RIE using O_2 gas etched away PI surrounding μLEDs.

Data availability

All data generated or analysed during this study are included in the paper.

40. Forrest, S. R., Bradley, D. D. C. & Thompson, M. E. Measuring the efficiency of organic light-emitting devices. *Adv. Mater.* **15**, 1043–1048 (2003).

Acknowledgements The team at Massachusetts Institute of Technology (MIT) acknowledges support from the National Science Foundation (award no. 2001231), the Defense Advanced Research Projects Agency Young Faculty Award (no. 029584-00001), the Air Force Research Laboratory (award no. FA9453-21-C-0717) and the US Department of Energy's Office of Energy Efficiency and Renewable Energy under the Solar Energy Technologies Office (award no. DE-EE0008558). The team at MIT also acknowledges support, in part, by LG electronics and Rohm Semiconductor. The team at Georgia Tech-Lorraine acknowledges partial funding by the French National Research Agency under the GANEXT Laboratory of Excellence project. The work by Y.J.H., J.J. and J.C. was supported by a National Research Foundation of Korea grant funded by the Ministry of Science and ICT (nos. 2018K1A4A3A01064272, NRF-2021R1A5A1032996 and 2022M3D1A2050793) and by the Ministry of Education (no. 2022R1A6C101A774).

Author contributions Jeehwan Kim, A.O., Y.J.H., K.C. and K. Lee conceived the idea and directed the team. J.S. coordinated and designed the experiments and characterization. H.K., S.S., J.J., B.-I.P., J.C. and K. Lu developed and performed epitaxial growth of red, blue and green LED films under the guidance of Jeehwan Kim, A.O. and Y.J.H. 2D material-coated substrates were prepared by H.K., S.S., J.J., B.-I.P., K. Lu, Y.L., K.Q. and Jekyung Kim. T.K. developed Si TFTs under the guidance of K.J.Y. M.S. developed the set-up and codes for measurement of

luminance, EQE and radiation pattern under the guidance of V.B., and J.S., J.J., M.S. and J.H.K. collected the data. J.S., H.K., J.J., M.-K.S., K. Lu, S.K., J.L., J.M.S., J.-H.K., J.S.K. and D.L. carried out layer transfer and fabrication of LEDs. J.S. collected *I–V* curves, EL microscopy images and optical transmission spectra. H.K., S.S. and K. Lu performed EBSD and XRD analyses. XPS and AFM data were collected by K.S.K. EL spectra were obtained by J.S. and H.K. All SEM, EDX and STEM imaging and analyses were performed by C.S.C. J.M.S. designed all three-dimensional schematic illustrations. H.E.L., H.Y., Y.K., H.S.K., S.-H.B. and K. Lee provided feedback throughout experiments and data analysis. The manuscript was written by J.S., H.K., S.S., J.J., Y.J.H., A.O. and Jeehwan Kim. All authors contributed to the analysis and discussion of results leading to the manuscript.

Competing interests The authors declare no competing interests.

Additional information

Supplementary information The online version contains supplementary material available at https://doi.org/10.1038/s41586-022-05612-1.

Correspondence and requests for materials should be addressed to Kyusang Lee, Kwanghun Chung, Young Joon Hong, Abdallah Ougazzaden or Jeehwan Kim.

Peer review information *Nature* thanks Kazuhiro Ohkawa and the other, anonymous, reviewer(s) for their contribution to the peer review of this work.

Reprints and permissions information is available at http://www.nature.com/reprints.

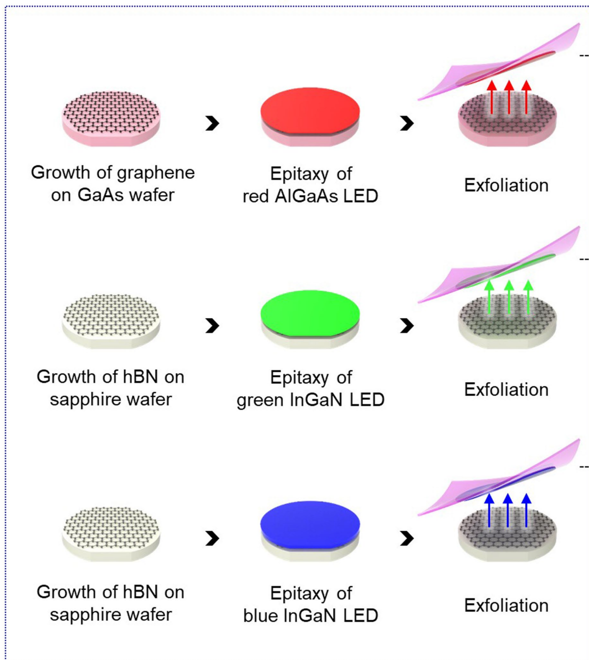

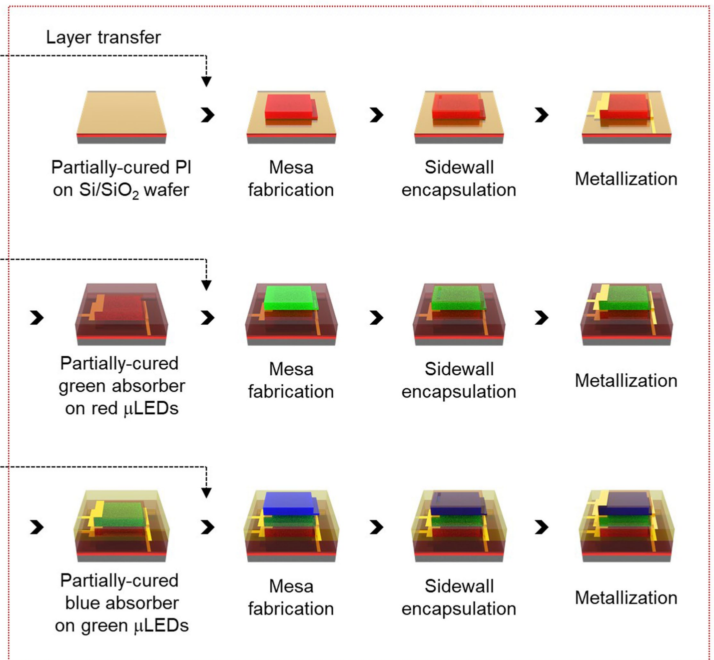

Extended Data Fig. 1 | Schematic illustrations of the 2D material-based layer transfer and vertical heterointegration process for constructing full-color vertical μLEDs. The layers are transferred and stacked in the order of red, green, and blue LEDs using polyimide as adhesion layer.

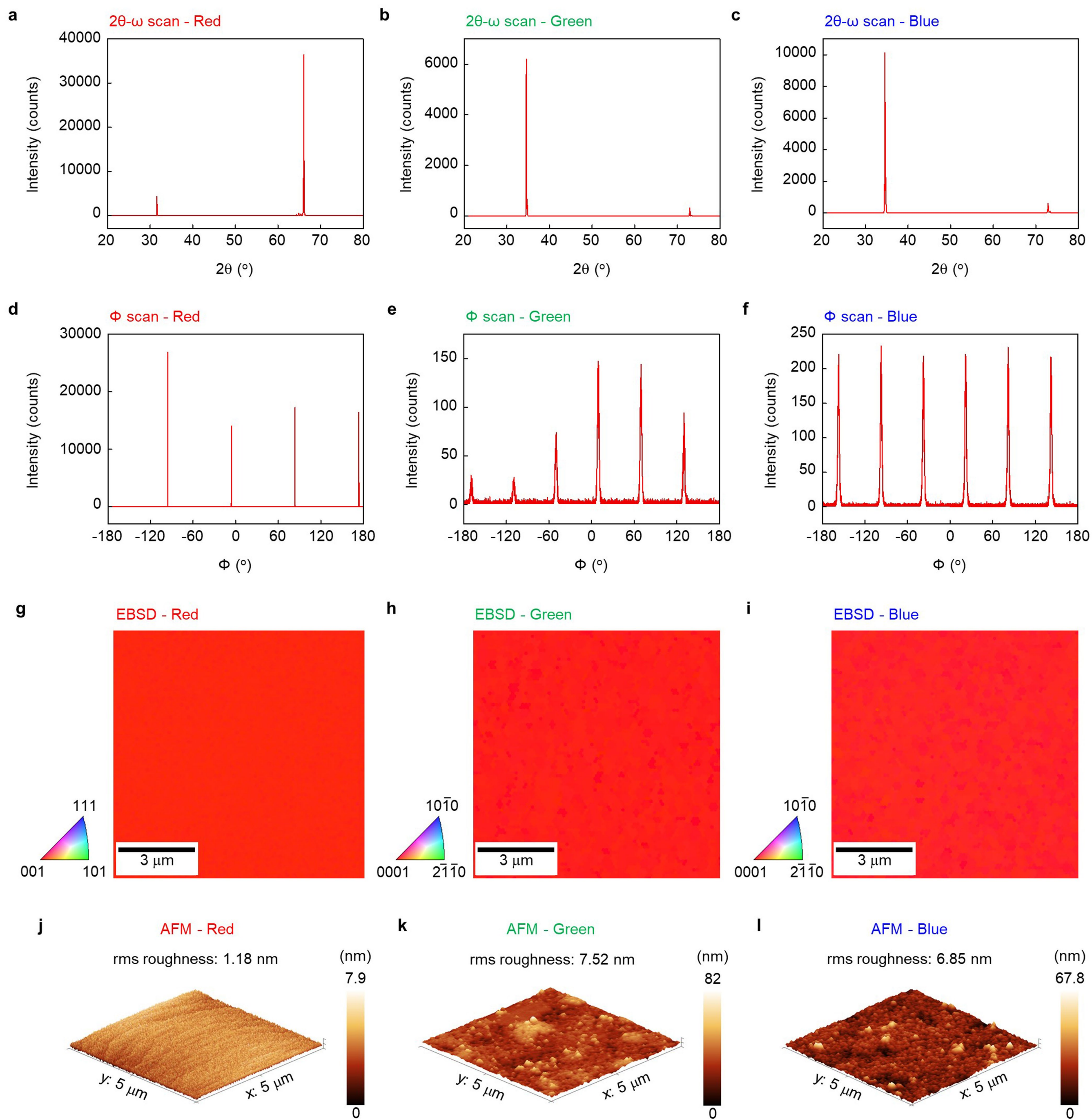

Extended Data Fig. 2 | XRD, EBSD, and AFM measurements of ultrathin RGB LED films obtained via 2DLT. a-c, XRD 2θ-ω scan results for red (a), green (b), and blue (c) LED films. **d-f**, XRD Φ scan results for red (d), green (e), and blue (f) LED films. **g-i**, EBSD analysis results for red (g), green (h), and blue (i) LED films. **j-l**, AFM morphology images for red (j), green (k), and blue (l) LED films.

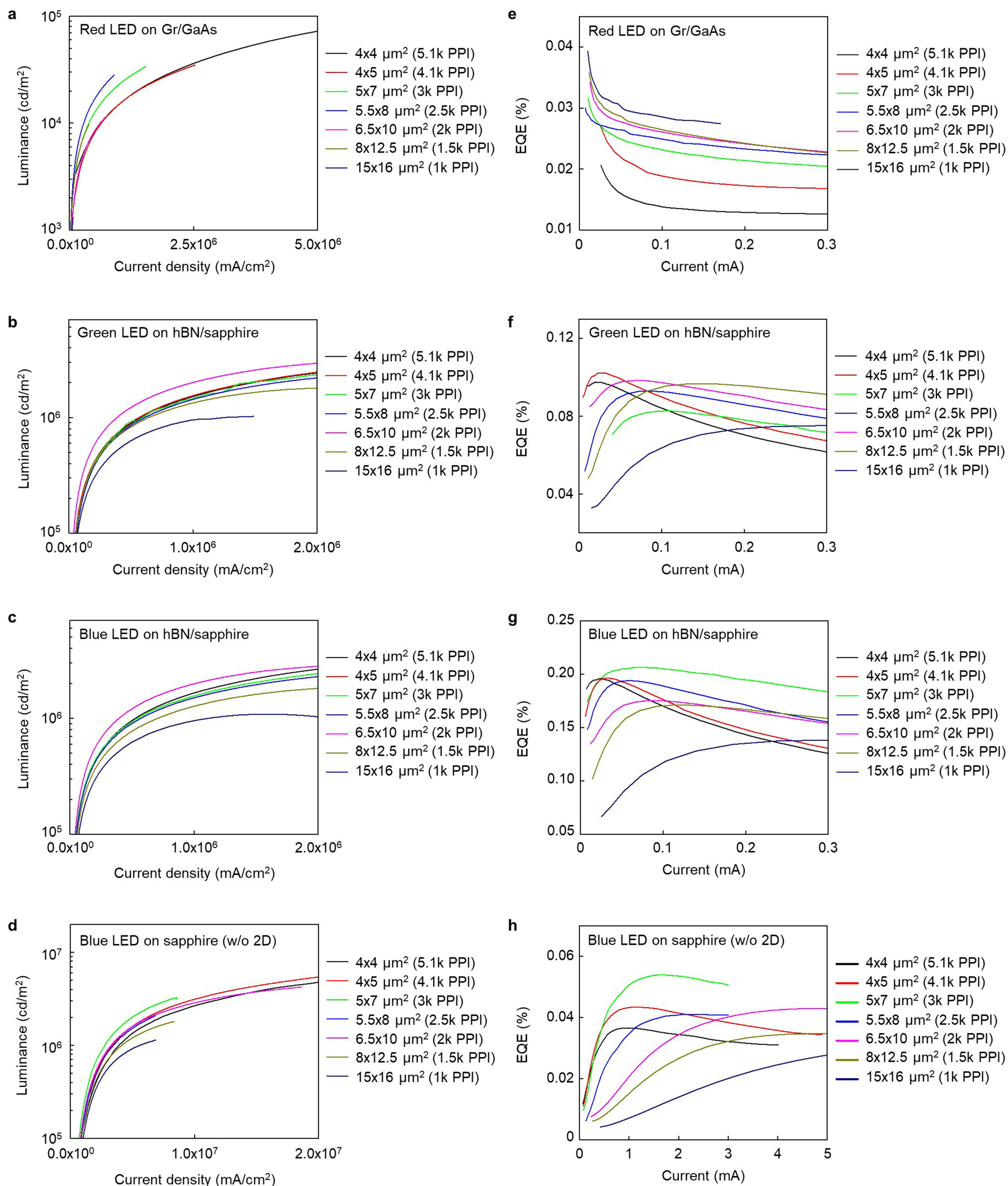

Extended Data Fig. 3 | Luminance and external quantum efficiencies (EQEs) of RGB μLEDs. a-d, Measured luminance of red (a), green (b), blue (c), and reference (d) μLEDs of varying size. **e-h**, Measured EQEs of red (e), green (f), blue (g), and reference (h) μLEDs of varying size. Red, green, and blue μLEDs are obtained via 2DLT, while reference devices are blue μLEDs grown directly on sapphire substrate without 2D layer.

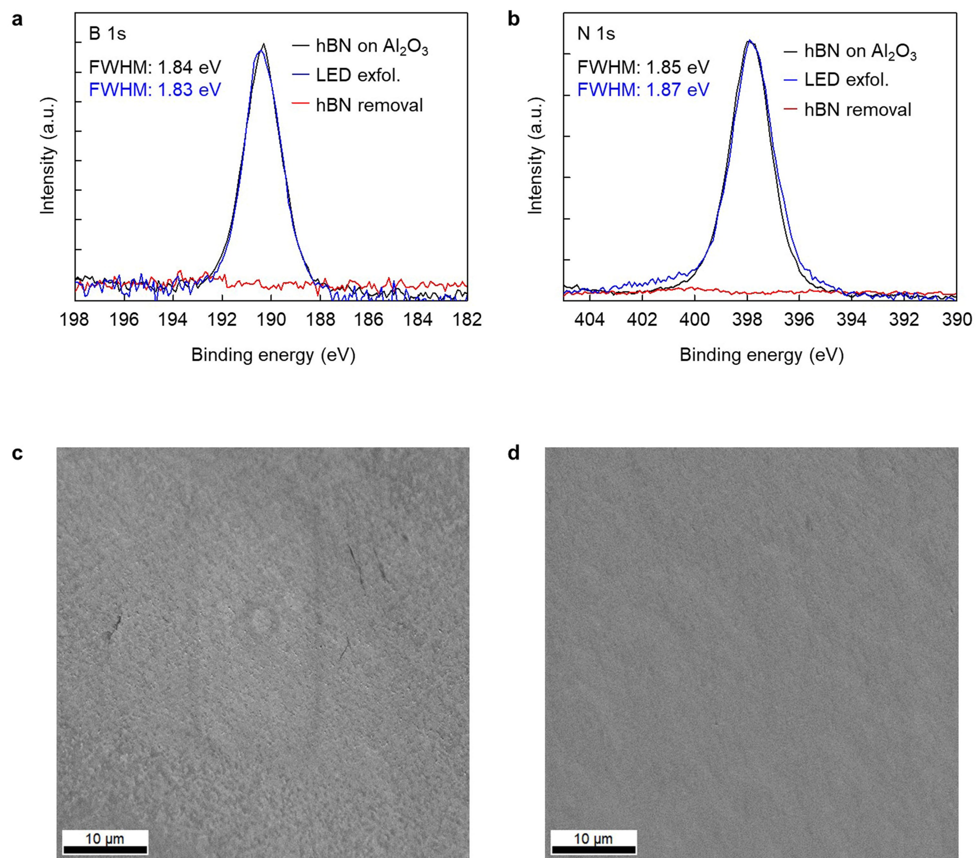

Extended Data Fig. 4 | Verification of reusability of sapphire substrates after 2DLT. a-b, XPS spectra of B 1*s* (a) and N 1*s* (b) regions for hBN-coated sapphire wafer (reference; black), used sapphire wafer following exfoliation of LED (LED exfol.; blue), and used sapphire wafer after removal of residual hBN layer (hBN removal; red). **c-d**, SEM images of blue LEDs on hBN grown on pristine (d) and reused (e) sapphire wafers.

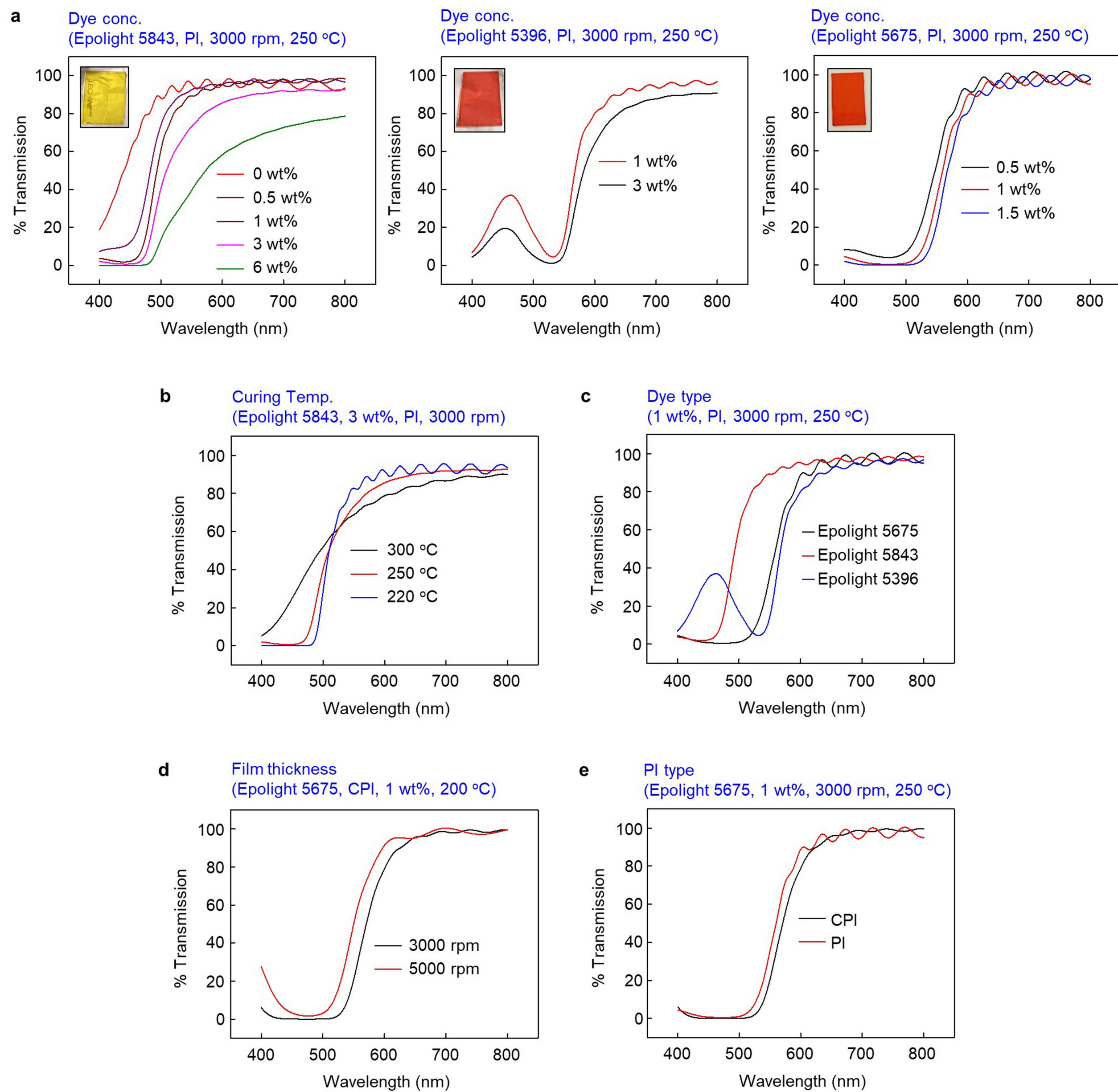

Extended Data Fig. 5 | Optimization of optical transmission characteristics of absorber interlayers. a-e, Optical transmission spectra obtained from absorber layers with varying concentrations of dyes dissolved in the PI precursor (a), film curing temperatures (b), types of dye product (c), film thickness (represented as spin-coating rate) (d), and types of PI (colorless PI from Kolon, Inc. and PI-2545 from HD Microsystems, Inc.) (e). Parameters in parentheses represent conditions that apply for all data in each plot. (a, Insets) Photographs of representative absorber layers coated on glass slide.

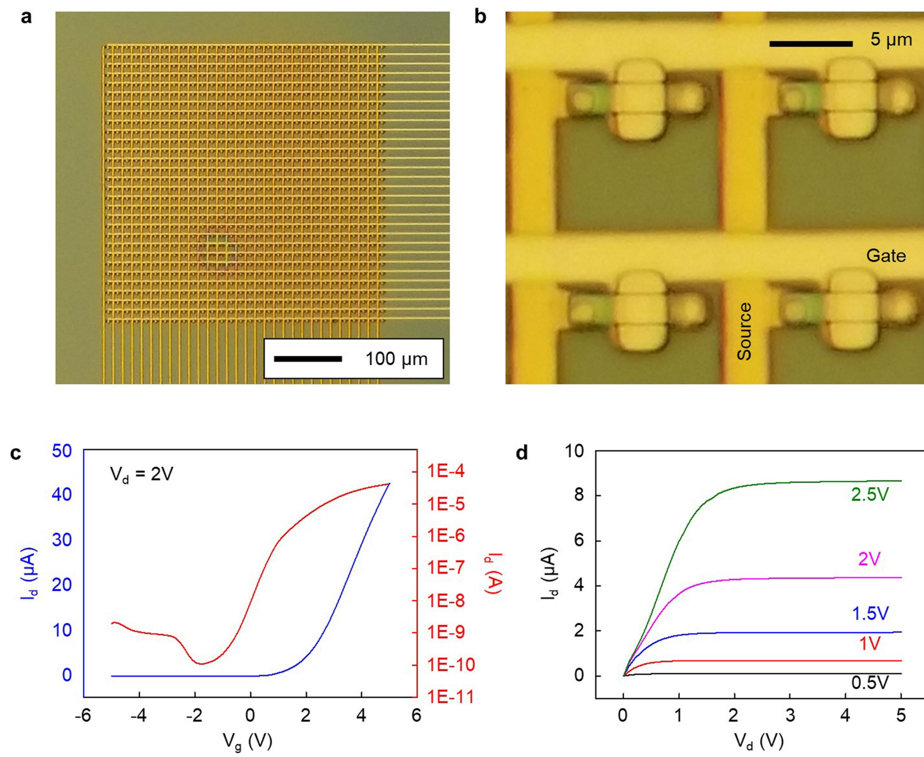

Extended Data Fig. 6 | Si TFTs on silicon-on-insulator wafer. a, **b**, Optical microscopy images of a 30 × 30 array of silicon TFTs fabricated on silicon-on-insulator wafer. Each TFT has dimensions of 2.2 µm × 9.2 µm. **c**, Transfer characteristics of the silicon TFT with W/L of 1.5 µm/2.2 µm, driven at V_{DS} of 2 V. **d**, Output characteristics of a Si TFT showing current saturation at V_{GS} values ranging from 0.5 V to 2.5 V.

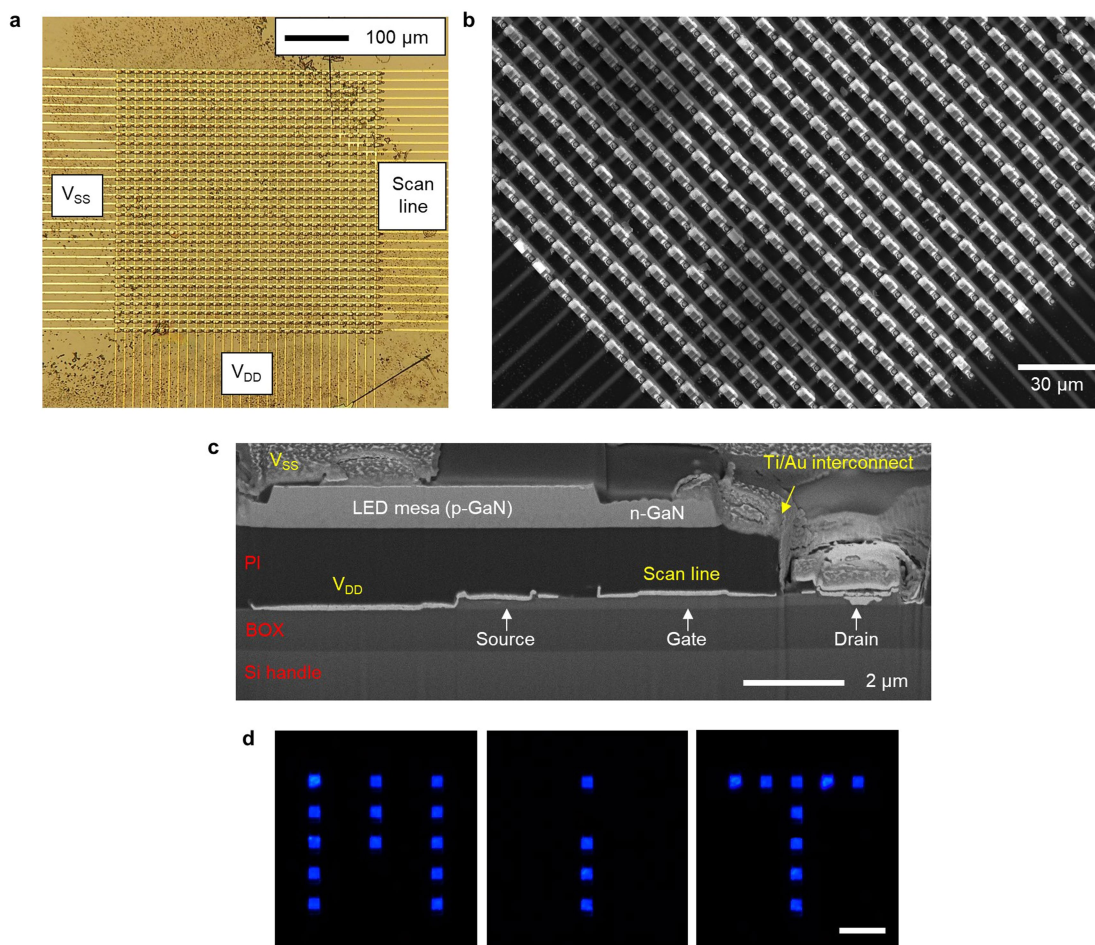

Extended Data Fig. 7 | Si TFT-integrated blue InGaN μLEDs. a, **b**, Optical microscopy and tilted SEM images of a 30 × 30 array of blue μLEDs vertically integrated with silicon TFTs. **c**, Cross-sectional SEM image of a blue μLED transferred on a 300 nm-thick silicon TFT on silicon-on-insulator wafer by PI adhesive layer and electrically interconnected by sputtered metal. **d**, Optical images of the active matrix μLED display displaying the 'mit' logo. Scale bar, 200 μm.

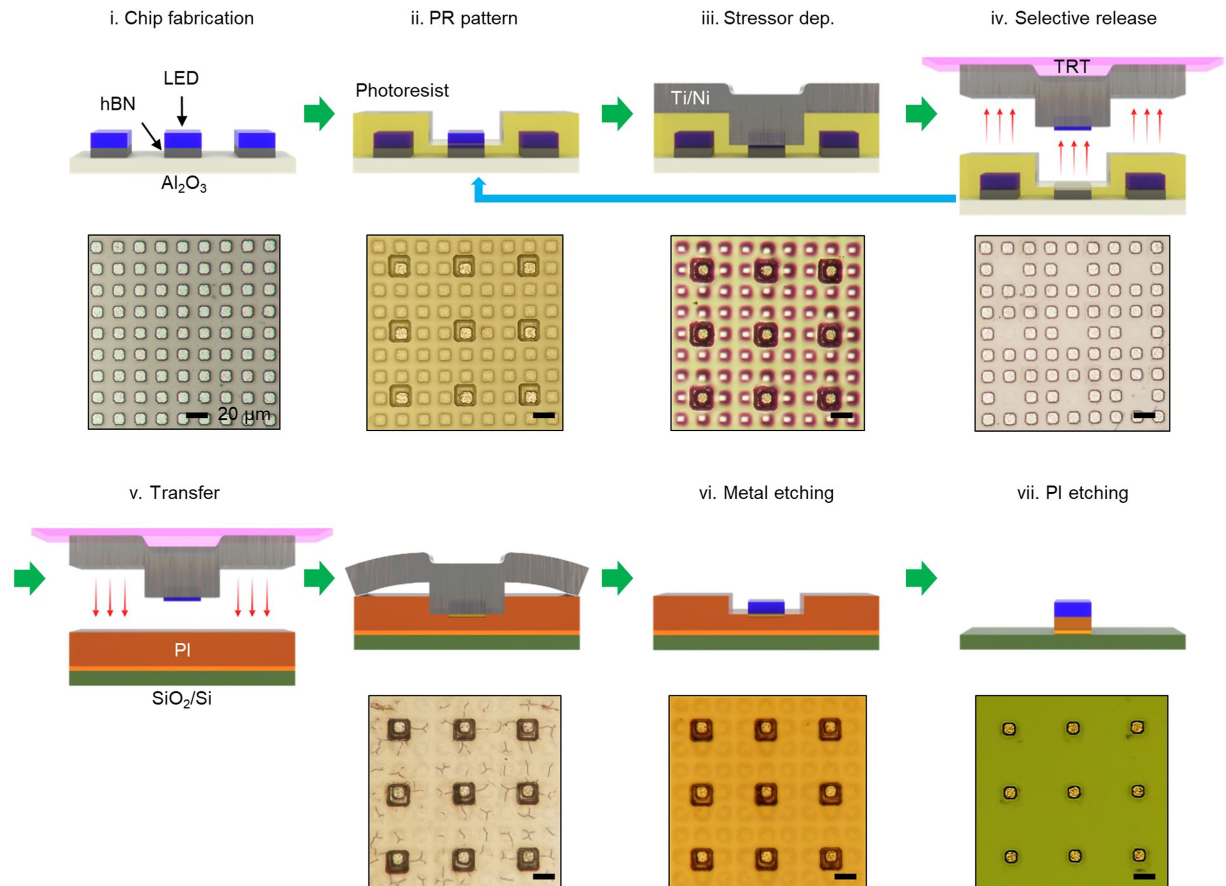

Extended Data Fig. 8 | Schematic illustrations and optical microscope images of 2DLT-based, selective μLED mass transfer process for manufacturing large-scale displays. The process involves the fabrication of blue LED chips (size ~10 μm) on hBN-coated sapphire substrate (step i), photolithography of a partially-developed photoresist (PR) pattern that exposes only the upper bodies of μLEDs to be transferred (step ii), deposition of Ni stressor layer and attachment of handling tapes (step iii), and mechanical lift-off of the exposed μLEDs via cleavage through the hBN layer (steps iv), which leaves behind the PR-coated chips on sapphire substrate that can undergo cleaning and additional lift-off (step ii). The slippery surface of 2D materials, combined with photolithography-based selection approach, enables facile yet highly resolved extraction of μLED chips among a densely-packed array (chip-to-chip separation ~10 μm). Cleaning the PR residue, transferring the μLEDs onto a secondary substrate, and removing Ni and underlying PI layers complete the process (steps v-vii).

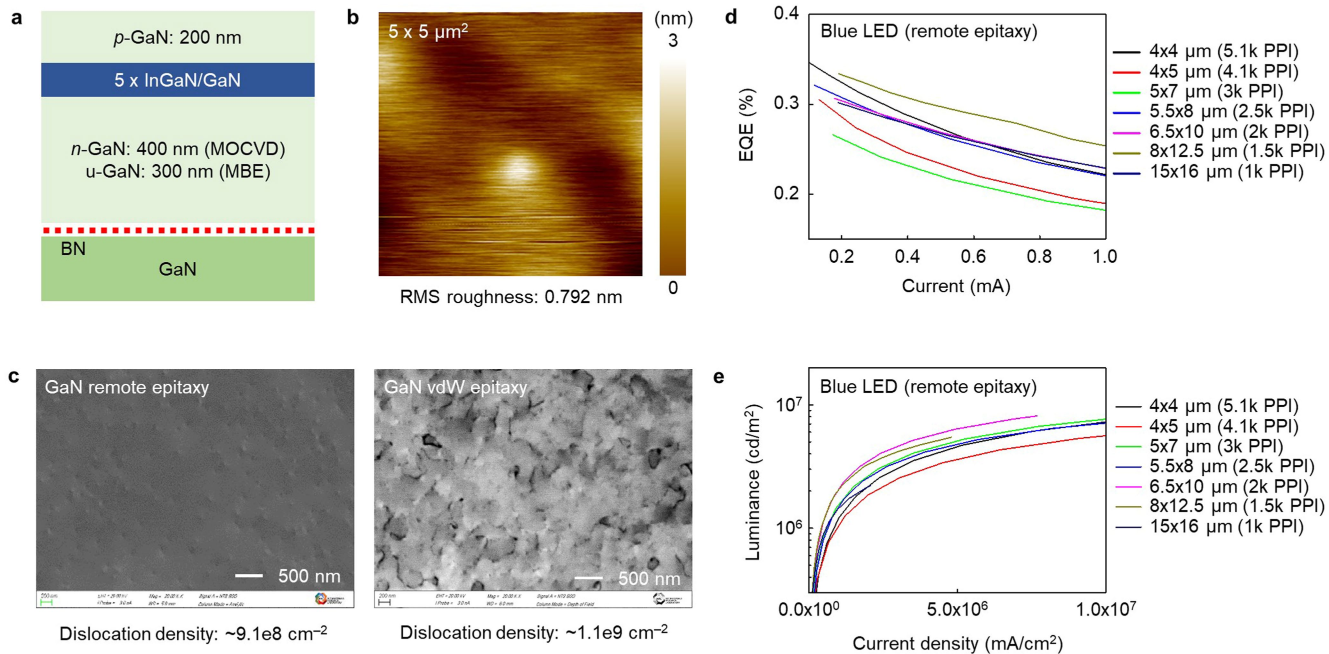

Extended Data Fig. 9 | Blue LED grown via remote epitaxy on GaN wafer. **a**, Schematic illustrations of the epitaxial structures of InGaN-based blue LED grown on GaN wafer. **b**, AFM morphology image of a GaN film grown via remote epitaxy. **c**, SEM images of the surfaces of GaN films grown via remote (left) and van der Waals (right) epitaxy techniques. **d**-**e**, Measured EQEs and luminance of blue μLEDs of varying size grown on GaN substrate.

Extended Data Table 1 | Benchmark of vertically-stacked and laterally-assembled μLED displays

Type		Journal (Year)	Stack height (μm)	Subpixel size (μm²)	Pitch (μm)	PPI
Vertical	Full color	*Opt. Express* 17, 9873–9878 (2009)	~450	500 × 500	n/a	n/a
		IEEE Trans. Electron Devices 60, 333–338 (2013)	~450	1000 × 1000	n/a	n/a
		Opt. Lett. 45, 6671–6674 (2020)	~450	780 × 780	n/a	n/a
		Proc SPIE 11310, 113100Z-1 (2020)	n/a	n/a	5 × 5	5000
		PNAS 118, e2023436118 (2021)	45	125 × 180	n/a	n/a
		Adv. Mater. Interfaces 8, 2100300 (2021)	~30	1000 × 1000	n/a	n/a
		Our study	**~9**	**4 × 4**	**5**	**5100**
	Dual color	*ACS Appl. Mater. Interfaces* 6, 19482–19487 (2014)	12.6 (B+Y)	260 × 260	n/a	n/a
		Opt. Express 25, 2489–2495 (2017)	n/a (G+B)	75 × 75	100	n/a
		Sci. Rep 7, 10333 (2017)	17.7 (R+G)	1000 × 500 (subpixel)	n/a	n/a
Lateral	Full color	*JDT* 12, 742–746 (2016)	-	250 × 250	1000	n/a
		Photonics Res. 5, A23–A29 (2017)	-	8 × 15	100 (RGB)	254 (RGB)
		ACS Photonics 5, 4413–4422 (2018)	-	1000 × 500	n/a	n/a
		Appl. Opt 58, 8383–8389 (2019)	-	100 × 250	500	n/a
	Full color (Mono color + CC)	*Photonics Res.* 5, 411–416 (2017)	-	35 × 35	40	~635 (mono)
		IEEE Photon. Technol. Lett. 30, 262–265 (2018)	-	30 × 30	n/a	n/a
		Nat. Photonics 15, 449–455 (2021)	-	1 × 1	n/a	8500 (mono), 300 (RGB)
		Nat. Nanotechnol 17, 500–506 (2022)	-	10 × 10	50 × 50	508 (mono)
	Mono color	*Appl. Phys. Lett.* 99, 031116 (2011)	-	12 × 12	15	1690
		Proc. SPIE 10104, 1010422-1 (2017)	-	8 (circle)	10	2540
		Nat. Nanotechnol 16, 1231–1236 (2021)	-	10 (circle)	n/a	1270

These include mono, dual, and full-colour μLED displays, as well as full-colour displays based on mono colour μLEDs coated with colour conversion (CC) layers.